Mathematical Modelling and Analysis
Volume 29, Issue 4, 767–780, 2024
https://doi.org/10.3846/mma.2024.20022

The Inverse Problem of Determining Profiles of Electrophysical Parameters in Eddy-Current Structuroscopy Using Apriori Information on Multifrequency Probing

Volodymyr Ya. Halchenko, Ruslana Trembovetska, Volodymyr Tychkov and Nataliia Tychkova

Cherkasy State Technological University
Blvd. Shevchenka 460, 18006 Cherkasy, Ukraine
E-mail: v.halchenko@chdtu.edu.ua
E-mail: r.trembovetska@chdtu.edu.ua
E-mail(*corresp.*): v.tychkov@chdtu.edu.ua
E-mail: n.b.tychkova.asp21@chdtu.edu.ua

Received September 27, 2023; accepted July 4, 2024

Abstract. Based on the proposed methodology, the essence of which is to identify the profiles of electrophysical parameters of planar objects of eddy-current testing by means of surrogate optimization in the active PCA-space of reduced dimensionality, the effectiveness of the approach is proved by modeling the process of measurement control using apriori accumulated information about an object, in particular, multifrequency probing. The particularity of these studies is the consideration of previously collected information not only on profile variations, but also on the effect of various object probing frequencies on the signal of the surface probe. The functions of the storage device and information carrier were performed by a neural network metamodel, characterized by a high computational efficiency. Numerical experiments have determined the accuracy indicators of the proposed improved method for determining the distributions of magnetic permeability and electrical conductivity along the subsurface layer of a metal object with changes in a microstructure. The analysis of the modeling results indicates a significant reduction in the level of computational resources required to solve the problem and an increase in the accuracy of profile identification.

Keywords: profiles of magnetic permeability and electrical conductivity, eddy current measurement control, multifrequency probing, apriori information, surrogate optimization, active subspace, metamodel, deep neural networks.

AMS Subject Classification: 65K02.

1 Introduction

Eddy current structuralscopy is a specific type of non-destructive testing of products and materials, which is characterized by the use of mathematical modeling both at the preparatory stage and during the measurement operations. It is due to a considerable difficulty in determining structure-dependent parameters, in particular magnetic permeability (MP) and electrical conductivity (EC), directly during physical measurements as not their integral values for the test objects (TO) are recorded, but, accordingly, their distributions in the subsurface layer of the object material, i.e., their profiles. The simultaneous reconstruction of both of profiles of electrophysical parameters based on the results of a single measurement by an eddy-current probe (ECP) allows, based on the relationships between electromagnetic properties and microstructural changes in metals, to draw conclusions about the purity of their composition, the state of heat treatment, the state of internal stress, hardness, temperature, etc. Thus, due to the extreme importance of ensuring product quality and normal trouble-free operation of equipment, the problem is relevant for many industries and has always been the focus of researchers' attention [1, 13]. The problem is quite extraordinary, belongs to the incorrectly posed ones and can be classified as an inverse measurement problem.

The general current state of research conducted in this area is analyzed in detail by the authors in [7, 17], where the main directions for further improvement of approaches are identified. However, there has recently been a tendency to use physical multi-frequency measurement techniques and their specific varieties, that makes it possible to obtain more additional information on the interaction of the electromagnetic field of probes exciation with the TO [9, 14, 15], which is one of the methods to improve the conditions for solving the inverse problem. The swept-frequency measurements in time are used with the same purpose [11, 22, 23]. A main disadvantage of these approaches is a drastic complexity of physical measurements, and, accordingly, signal processing algorithms, and the increased time to establish testing results. However, the advantages of this approach can be achieved without conducting a series of physical measurements directly on the TO if the collection and accumulation of additional apriori information about the TO is transferred to the modeling stage, preceding the measurement procedures, and stores it in the metamodel [7]. In addition, another function of the metamodel is a high-performance, without time spending calculation of the ECP signal, which is used as a component for constructing the target function within the framework of the proposed surrogate optimization method for solving the problem under study.

Thus, the aim of the article is to reseach, by means of computer simulation, the process of eddy-current determination of profiles of material properties of planar test objects based on the implementation of surrogate optimization in an active compact subspace of reduced dimensionality using apriori accumulation of information in the metamodel obtained by preliminary simulation with varying profiles and multifrequency modes of operation of probes.

The advantages of the proposed method are: simultaneous determination of

profiles for one measurement at one fixed frequency when taking into account the hidden patterns of the ECP signal formation in the metamodels, which take into account, in addition to electrophysical parameters, the influence of sensing frequencies; reduction of errors in profile reconstruction compared to studies where only EC and MP were taken into account in metamodels at a fixed ECP excitation frequency; simplification of the conditions for finding an extremum by an optimization algorithm and obtaining better solution values compared to the search in the full-factor space by using the method PCA (Principal Component Analysis) to reduce the dimensionality of metamodels.

Thus, the paper proposes a method for simultaneous reconstruction of the EC and MP profiles of planar conductive objects under testing based on the implementation of surrogate optimization in an active compact subspace of reduced dimensionality obtained by linear transformations, with apriori accumulation of information in metamodels obtained by advance modeling with profile variation and multifrequency sensing modes.

2 Research methodology

The proposed research methodology is as follows. The measurement process for reconstructing of the electrophysical parameters profiles of the TO is based on solving an optimization problem using surrogate modeling techniques. In other words, a single measurement of the EMF (electromotive force) ECP is provided when controlling a planar TO. It results in the recorded values of the signal amplitude and phase, which for further calculations can be conveniently represented in the algebraic form of a complex number. Then, $e_{\text{mes}} = C_{\text{mes}} + jD_{\text{mes}}$, where C_{mes} and D_{mes} are the real and imaginary parts of the measured EMF, respectively. Mathematically, the task of reconstructing the EC and MP profiles is to minimize the following quadratic function, which is the target function in the optimization algorithm:

$$F(\boldsymbol{\sigma}, \boldsymbol{\mu}, f) = (C_{\text{mes}} - G_{\text{metamod}})^2 + (D_{\text{mes}} - Z_{\text{metamod}})^2 \to \min, \qquad (2.1)$$

where $e_{\text{metamod}} = G_{\text{metamod}} + jZ_{\text{metamod}}$, is calculated using a high-performance neural network metamodel [6] for the electrodynamic model e_{mod}, which depends on the desired profiles of electrical conductivity and relative magnetic permeability, represented in a discretized form by the corresponding vectors $\boldsymbol{\sigma}$, $\boldsymbol{\mu}$ of dimension L each, and f – the excitation frequency of the ECP at which the measurement is performed. Moreover, L denotes the number of conditional discretization layers of the continuous distribution of electrophysical parameters along the thickness of the TO. The desired parameters in the optimization are the components of the EC and MP vectors, on the values of which the value of the right-hand side of the target function (2.1) depends.

On account of the problem specifics, which is an ill-posed one, the topology of the hypersurface of the target function response has a problematic topology with multidimensional ravines for finding the optimum. To overcome these obstacles, it is necessary to use global optimization algorithms, in particular, gradientless stochastic algorithms. In view of this, the search for an extremum

of the target function is performed using a heuristic bionic stochastic global optimization algorithm, namely a hybrid multiagent particle swarm optimization algorithm with evolutionary formation of the swarm composition [8].

The next key point in identifying profiles is the creation of a metamodel characterized by a high accuracy of approximation of the response hypersurface, determined by a highly nonlinear analytical functional dependence for calculating the EMF e_{mod}. This dependence is obtained by solving a boundary value problem based on Maxwell's equations with appropriate boundary conditions and is known as the Uzal-Cheng-Dodd-Deeds electrodynamic model [1,12,19]. It contains multiple convergent non-proprietary integrals of the first kind, with the subintegral function being a complex combination of cylindrical Bessel functions of the first kind of zero, first, and m-th orders of the complex argument. A feature of the model is the piecewise constant distribution of electrophysical parameters according to certain experimentally established laws for most technological processes.

2.1 Electrodynamical model

Previous articles by the authors [3,17] contain information on the thorough verification of a software product implemented on the basis of the analytical electrodynamic model Uzal-Cheng-Dodd-Deeds as interpreted by Theodoulidis [16] for a conditionally multilayered representation of TO, which is:

$$e_{\text{ mod }} = -j \cdot \omega \cdot w_{mes} \cdot \oint_{Lc} A(P) dl_p,$$

where:

$$A(r_\delta, z_\delta) = \int_0^\infty J_1(\kappa r_\delta) \cdot [C_s \cdot e^{\kappa z_\delta} + D_{ec} \cdot e^{-\kappa z_\delta}] d\kappa,$$

$$C_s = \frac{\mu_0 \cdot i_0}{2} \cdot \frac{\chi(\kappa r_1, \kappa r_2)}{\kappa^3} \cdot (e^{-\kappa z_1} - e^{-\kappa z_2}),$$

$$D_{ec} = \frac{(\kappa\mu_{t+1} - \lambda_1) V_{11}(1) + (\kappa\mu_{t+1} + \lambda_1) V_{21}(1)}{(\kappa\mu_{t+1} + \lambda_1) V_{11}(1) + (\kappa\mu_{t+1} - \lambda_1) V_{21}(1)} C_s,$$

$$i_0 = WI(r_2 - r_1)^{-1} \cdot (z_2 - z_1)^{-1},$$

$$\chi(x_1, x_2) = \left\{ x_1 J_0(x_1) - 2 \sum_{m=0}^{\infty} J_{2m+1}(x_1) \right\} - \left\{ x_2 J_0(x_2) - 2 \sum_{m=0}^{\infty} J_{2m+1}(x_2) \right\},$$

$$V(1) = T(1,2) \cdot T(2,3) \cdots T(L-2, L-1) \cdot T(L-1, L),$$

$$T_{11}(t, t+1) = \tfrac{1}{2} e^{(-\lambda_{t+1} + \lambda_t) dt} \left(1 + \left(\mu_t / \mu_{t+1}\right)\left(\lambda_{t+1} / \lambda_t\right)\right),$$

$$T_{12}(t, t+1) = \tfrac{1}{2} e^{(\lambda_{t+1} + \lambda_t) dt} \left(1 - \left(\mu_t a / \mu_{t+1}\right)\left(\lambda_{t+1} / \lambda_t\right)\right),$$

$$T_{21}(t, t+1) = \tfrac{1}{2} e^{(-\lambda_{t+1} - \lambda_t) dt} \left(1 - \left(\mu_t / \mu_{t+1}\right)\left(\lambda_{t+1} / \lambda_t\right)\right),$$

$$T_{22}\,(t,t+1) = \tfrac{1}{2} e^{(\lambda_{t+1}-\lambda_t)dt}\left(1+\left(\mu_t/\mu_{t+1}\right)\left(\lambda_{t+1}/\lambda_t\right)\right),$$
$$\lambda_t = \left(\kappa^2 + j\cdot\omega\cdot\mu_0\cdot\mu_t\cdot\sigma_t\right)^{\frac{1}{2}}.$$

$A(r_\delta, z_\delta)$ is the azimuthal component of the vector potential, Wb/m; $\mathbf{V}(1)$ – a matrix, whose elements are V_{11}, V_{21}; $\mathbf{T}()$ – matrix with elements $T_{11}()$, $T_{12}()$, $T_{21}()$, $T_{22}()$; $\mu_0 = 4\cdot\pi\cdot 10^{-7}$ is the magnetic constant in vacuum, H/m; $J_m()$ – cylindrical Bessel functions of the first kind of m-th order, $m = 0, 1, \ldots$; r_δ, z_δ are the coordinates of the observation point P in the cylindrical coordinate system, m; $(r_2 - r_1)$ is the width of the cross-section of the ECP excitation coil, m; $(z_2 - z_1)$ is the height of the cross-section of the ECP excitation coil, m; w_{mes} is the number of turns of the ECP measuring coil; e_{mod} is the EMF induced in the ECP measuring coil, V; Lc is the contour of the ECP measuring coil; t is the current number of the conditional layer out of L possible; μ_t, λ_t are, respectively, the relative magnetic permeability and the computational parameter of the t-th conditional layer.

2.2 Creating metamodel

A neural network metamodel (surrogate model) is created using the specified software product. It is rather difficult to approximate the model dependence due to its significant nonlinearity. To avoid creating a complex-valued neural network, we split it into two real-valued deep neural networks with common inputs in the form of $\boldsymbol{\sigma}$ and $\boldsymbol{\mu}$ and f, and separate outputs for the real and imaginary parts of the EMF modeled by the electrodynamic model. Taking into account the generalizing ability of neural networks, the metamodel determines the characteristic behavior of the ECP output signal in accordance with changes in these inputs during training. To ensure a high accuracy of the electrodynamic model approximation by the surrogate, the nodal points of hyperspace at which the EMF was calculated by the electrodynamic model were determined according to a computerized uniform DOE (design of experiment) [2, 10]. In this study, a design based on a set of modified LP_τ-quasi-Sobols sequences was used, which is characterized by low discrepency values both in the volume of the hyperparallelepiped of the search space and in 2D projections [4].

This makes it possible to place nodal points with a fairly high probability in such places of hyperspace where complex changes in the behavior of the multidimensional response surface are observed [21].

2.3 Surrogate optimization in an active compact subspace

Finally, we also specify that the optimization algorithm for this problem is characterized by a large number of variables. This is due to the need to split the subsurface layer of the TO into conditional layers with a sufficiently high discreteness in order to obtain realistic piecewise constant analogs of continuous profiles of electrophysical parameters. An increase in the number of search variables, i.e., the dimensionality, in surrogate optimization problems leads to the costly creation of a metamodel, requiring an increase in the sample of training data. In addition, under these conditions, the "curse of dimensionality" begins to manifest itself in optimization with the corresponding significant

consequences for the accuracy of the search for an extremum. Therefore, the creation of the metamodel and optimization is performed in a low-dimensional representation of the design space, i.e., the active subspace, which is actually an encapsulation of the high-dimensional space into its compact representation [18]. To do this, we use the PCA method, which allows us to find the main directions in a high-dimensional space that have the greatest impact on data variation by linear transformations.

Consequently, the dimensionality of the space can be reduced while retaining a significant part of the complete information [20]. It should also be noted that the actions in the algorithm with the variables contained in the target function and represented in the normalized form are quite decisive in the proposed approach. This eliminates a significant difference of six orders of magnitude in the values of the desired EC and MP indicators during the search for the optimum, which allows the optimization algorithm to work adequately. The back projection from the PCA space of the principal components to the original space is performed to obtain the actual profiles after the optimization is completed. Finally, it should be noted that due to the stochastic nature of the applied optimization algorithm, the multi-start technique was used to eliminate the relevant problems in the study, followed by averaging the obtained variants of the electrophysical parameter profiles.

3 Numerical experiments

The construction of metamodels by means of the DNN is based on a large sample size, which is calculated at the points of the multidimensional DOE [4] based on LP$_\tau$-Sobols sequences. As it has been noted above, the study takes into account three factors $\boldsymbol{\sigma}$, $\boldsymbol{\mu}$ and f when creating a metamodel, then to implement a homogeneous DOE, a combination of LP$_\tau$-sequences ξ_1, ξ_6, ξ_{14} is used, which provides acceptable indicators of centered CD and wrap-around WD, mixed MD, and weighted symmetrized centered WSCD discrepancies [4], which together indicate the homogeneity of the created DOE. This design creation is due to the much higher accuracy of the hypersurface response approximation.

Figure 1(a) shows such a DOE on a unit scale on the LP$_\tau$-Sobols sequences ξ_1, ξ_6, ξ_{14} with improved homogeneous two-dimensional projections. The total number of DOE points is equal to $N_{profile} = 8191$, but for the convenience of visualizing the homogeneity of the DOE, only a limited number of them, namely 128, are shown in Figure 1. In addition, the perfection of the created design can be assessed using Voronoi diagrams by the area of each formed segment of the diagram Figure 1(b).

On the basis of the generated DOE, a scaling transition from a unit cube to a parallelepiped of the real factor space was made. Usually, the profiles are controlled for compliance with the ideal distribution of electrophysical parameters characteristic of the primary technological processes. However, minor deviations of the profiles from the ideal ones within certain technological tolerances are also considered normal. Therefore, the dimensions of the parallelepiped were determined within the technological tolerance $\delta T = \pm 15\%$ relative to the ideal values of the profile parameters on the TO surface with a maximum change

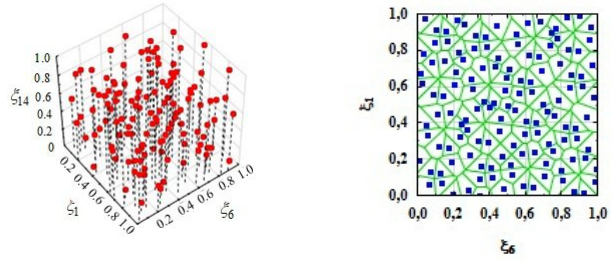

a) b)

Figure 1. Visualization of a homogeneous three-factor DOE: (a) spatial representation; (b) one of the two-dimensional projections (ξ_1,ξ_6) of the design.

in them. The boundary numerical values of the electrophysical parameters of the EC and MP at the DOE points in the real factor space are given in Table 1. Note that σ is measured in S/m. In this case, the ideal profile is the profile of the EC, the minimum and maximum values for which are $\sigma_{\min} = 2 \times 10^6$ S/m, $\sigma_{\max} = 9.2 \times 10^6$ S/m, and for the MP profile – $\mu_{\min} = 1$, $\mu_{\max} = 26.1$, respectively (for example, point 1 of the DOE in Table 1). Then, the ranges of change in the EC parameters, taking into account 15% of the technological tolerance, will be $7.82 \times 10^6 \le \sigma_{\max} \le 10.1 \times 10^6$ S/m; and MP – $22.185 \le \mu_{\max} \le 30.015$, with $\sigma_{\min}$ and $\mu_{\min}$ being unchanged for any profile, since they characterize the TO material in the zone without microstructural changes.

In addition to the values of the electrophysical parameters, the creation of the DOE requires knowledge of the range of changes in the excitation current frequency $1 \le f \le 20$ kHz, which is informative for observing the signal response at different depths of penetration of the EMF probing. Within the limits

Table 1. Initial data for the creation of DOE for the three-factor space.

DOE point	Design in a unit cube			Design in real space		
	ξ_1	ξ_6	ξ_{14}	$\sigma_{\max} \times 10^6$, S/m	$\mu_{\max}$	f, kHz
1	0.5	0.5	0.5	9.2	26.1	10.5
2	0.25	0.75	0.75	9.89	24.1425	15.25
3	0.75	0.25	0.25	8.51	28.0575	5.75
4	0.125	0.125	0.125	8.165	23.1638	3.375
5	0.625	0.625	0.625	9.545	27.0788	12.875
...	...	...	...	...	...	...
8188	0.249878	0.379761	0.497925	8.868248	24.1417	10.4601
8189	0.749878	0.879761	0.997925	10.24825	28.0567	19.9601
8190	0.499878	0.629761	0.747925	9.558248	26.0992	15.2101
8191	0.999878	0.129761	0.247925	8.178248	30.0142	5.7101

of change in the electrophysical parameters in real space indicated in Table 1, we calculated the distribution of the EC $\boldsymbol{\sigma}$ by the typical "exponent" approximation, and the distribution of the MP $\boldsymbol{\mu}$ by the "gaussian" approximation [19] for all DOE points, which corresponds to the number of profiles in the total

sample of Table 2. At the same time, to obtain piecewise constant profiles of electrophysical parameters, the thickness of the subsurface layer $D = 3 \cdot 10^{-4}$ m was a subject to a conditional division into $L = 60$ layers. For these "technological" profiles, the EMF values were calculated using the electrodynamic model (2.1). As a result, a data set of size $N_{profile} = (n_\mu \times n_\sigma)$ was obtained, where $n_\mu, n_\sigma = 60$ is the number of points of approximation of the MP and EC profiles (Table 2), to which the PCA method based on the SVD-decomposition was applied to reduce the dimensionality of the factor space. As a result of the

Table 2. Training sample 8191 × 121 for creating a metamodel in the full factor space.

No	$\mathrm{Re}(e_{\mathrm{mod}})$	$\mathrm{Im}(e_{\mathrm{mod}})$	f,kHz	μ_1	...	μ_{60}	$\sigma_1 \times 10^6$,S/m	...	$\sigma_{60}, S/m \times 10^6$
1	-3.737	-3.111	10.5	1.0627	...	26.0969	8.834221	...	2.073403
2	-4.295	-3.051	15.25	1.0578	...	24.1396	9.490569	...	2.107756
3	-2.57	-2.872	5.75	1.0676	...	28.0546	8.177872	...	2.039050
4	-1.569	-2.22	3.375	1.0554	...	23.1610	7.849698	...	2.021873
5	-4.162	-3.151	12.875	1.0651	...	27.0755	9.162395	...	2.090580
...	...	...	...	...	...	...	...	...	...
8188	-3.671	-3.117	10.460	1.0578	...	24.1391	8.518648	...	2.056886
8189	-4.897	-3.154	19.960	1.0676	...	28.0534	9.831345	...	2.125592
8190	-4.441	-3.184	15.210	1.0627	...	26.0961	9.174997	...	2.091239
8191	-2.599	-2.974	5.710	1.0724	...	30.0106	7.862300	...	2.022533

SVD-decomposition, 62 influential factors in the active compact subspace were selected for which the eigenvalues are greater than 1. The matrix of parameters G in the active compact subspace of size $N_{profile} \times n_{active}$, where n_{active} = 62 is the number of variables **g** in this space (Table 3) is used to train deep MLP-neural networks (DNNs). Moreover, out of the total sample $N_{profile}$ = 8191, 73% of the profiles were allocated for training neural networks, which is N = 6012, which in turn were also distributed for training NNs $N_{traine} = 4206$, testing $N_{test} = 903$, and cross-validation $N_{CV} = 903$. The rest of the sample data did not participate in the training, but later some of them were used as simulation data obtained by the ECP measurements to check the reliability of the profile determination method.

Table 3. Training sample 8191 × 62 for creating a metamodel in active compact subspace.

No	g_1	g_2	g_3	...	g_{60}	g_{61}	g_{62}
1	-34344006	-40876.45	-0.0058198	...	-0.1760432	-0.5642135	0.0230887
2	-36406779	469672.51	4751.5623	...	-0.1381319	-0.2716042	0.3864101
3	-32281232	-551426.6	-4751.575	...	-0.3059848	-0.2270135	-0.167599
4	-31249845	-806701.2	-7127.3593	...	-0.4776733	-0.5156286	-0.232562
5	-35375392	214397.8	2375.7778	...	-0.217832	-0.0950621	0.3913253
...	...	...	...	...	...	...	...
8188	-33352224	-286351.9	-40.662234	...	0.0878661	-0.2773956	0.062138
8189	-37477772	734747.26	9462.4749	...	-0.066291	-0.2335911	-0.069082
8190	-35414998	224197.78	4710.9065	...	-0.177943	-0.4745465	-0.050073
8191	-31289451	-796901.5	-4792.2309	...	0.6592515	-0.1609488	0.2685339

The analysis of the average absolute error MAE (Mean Absolute Error), RMSE (Root Mean Square Error) and coefficient of determination R^2 in the selection of NN architectures shows the feasibility of using a DNN with four hidden layers, a hyperbolic tangent activation function in each hidden layer and the Levenberg-Marquardt learning method. Therefore, two real-valued deep neural networks with common inputs in the form of g-parameters and separate outputs for the real and imaginary parts of the EMF were created. As a result, we obtained networks with four hidden layers Re-MLP-13-13-12-11-1 for the real part of the EMF and Im-MLP-14-14-12-11-1 for the imaginary part with the corresponding number of neurons in them, as well as the network output. The validity of the obtained metamodels was evaluated by scatter plots and errors $MAPE_{metamod}$, % (Mean Absolute Percentage Error), separately for the training, cross-validation, and test samples, the results of which are shown in Figure 2. The obtained metamodels were verified by a number of

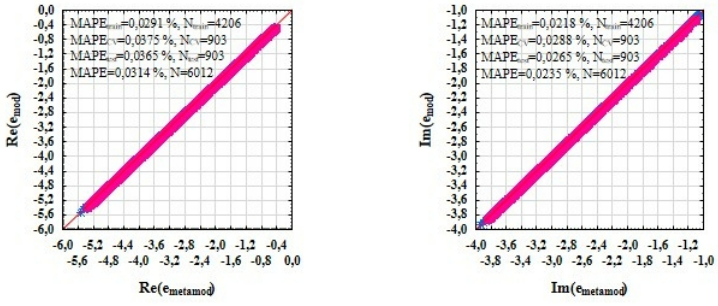

a) b)

Figure 2. Scatter plots of metamodels: (a) Re-MLP-13-13-12-11-1; (b) Im-MLP-14-14-12-11-1.

statistical indicators. According to the Fisher criterion, their adequacy and informativeness (Table 4 and Table 5) were checked at the level of significance of 5%. The obtained experimental values of Fisher's criterion significantly exceed its critical value for both metamodels, proving their adequacy. In addition to that, a large coefficient of determination is considerably significant according to Fisher's criterion and shows a high informativeness of the created metamodels.

Table 4. Analysis of the adequacy and informativeness of the Re-MLP-13-13-12-11-1 metamodel.

Average square of elements	Number of degrees of freedom	Adequacy	Informativeness
$MS_D = 156.40629$	$v_D = 62$	$F^{\text{total}}_{(62;5949)} =$	$R^2 = 0.9999$
MS_R=8.50126·10^{-7}	$v_R = 5949$	$\frac{MS_D}{MS_R} = 1.84 \cdot 10^8$	$F^{\text{total}}_{(62;5949)} =$
$MS_T = 1.613322$	$v_T = 6011$	$F^{\text{table}}_{(0.05;62;5949)}$=1.314	$\frac{R^2 v_R}{(1-R^2)v_D}$=1.89·10^6

Table 5. Analysis of the adequacy and informativeness of the Im-MLP-14-14-12-11-1 metamodel.

Average square of elements	Number of degrees of freedom	Adequacy	Informativeness
$MS_D = 30.58277$	$v_D = 62$	$F^{\text{total}}_{(62;5949)} =$	$R^2 = 0.99963$
$MS_R = 7.2247 \cdot 10^{-7}$	$v_R = 5949$	$4.23 \cdot 10^7$	$F^{\text{total}}_{(62;5949)} =$
$MS_T = 0.315558$	$v_T = 6011$	$F^{\text{table}}_{(0.05;62;5949)} = 1.314$	$2.63 \cdot 10^5$

To solve the inverse problem, a heuristic stochastic global optimization algorithm was applied, namely a hybrid multi-agent particle swarm optimization algorithm with evolutionary formation of the swarm composition. As noted earlier, in order to improve the accuracy of solutions, the multi-start technique was used in the study. Thus, a series of starts of the optimization algorithm were performed and thirty-nine solutions were obtained, inverse transformations were performed from the PCA-space principal component to the primary space, and actual MP and EC profiles were obtained for four test EMF measurements. The results of the errors $MAPE$, % of the profiles in each run are shown in Table 6.

Table 6. Relative error values for the reconstructed MP and EC profiles based on the results of starts of algorithm optimization.

	$MAPE$, %							
	e_{mes1}		e_{mes2}		e_{mes3}		e_{mes4}	
No	Re(e_{mes})=-1.579		Re(e_{mes})=-0.7463		Re(e_{mes})=-3.539		Re(e_{mes})=-2.267	
	Im(e_{mes})=-2.197		Im(e_{mes})=-1.474		Im(e_{mes})=-2.92		Im(e_{mes})=-2.73	
	$f = 3.2$ kHz		$f = 1.54$ kHz		$f = 9.64$ kHz		$f = 5.02$ kHz	
	μ	σ	μ	σ	μ	σ	μ	σ
1	0.466	0.918	5.072	3.008	1.992	0.292	3.113	3.38
2	1.874	0.617	5.099	2.986	0.898	0.221	2.389	0.813
3	0.436	0.814	2.482	1.441	1.216	1.318	1.238	2.05
4	1.854	0.638	4.456	1.852	3.346	0.219	5.293	1.653
5	3.964	3.04	2.679	1.936	2.021	0.756	1.508	1.143
6	0.184	2.901	2.089	1.547	2.046	0.724	3.789	2.038
7	3.623	1.478	2.472	1.188	2.541	1.992	6.057	4.106
8	1.375	0.412	1.703	3.329	1.795	1.621	4.012	3.743
9	1.327	0.623	2.509	1.894	2.136	0.999	1.509	2.551
10	0.669	0.807	4.038	3.065	1.604	1.572	2.4	4.075
⋮	⋮	⋮	⋮	⋮	⋮	⋮	⋮	⋮
34	4.027	0.27	0.794	0.636	1.762	1.451	10.019	3.859
35	2.309	0.785	3.238	2.451	3.438	1.144	2.561	1.281
36	2.918	1.885	2.256	0.791	0.329	0.951	1.321	1.798
37	3.627	4.487	2.849	2.759	0.636	0.93	1.761	2.642
38	5.421	1.648	1.436	3.951	1.987	0.574	3.814	0.553
39	4.87	2.082	2.412	2.978	7.499	3.813	9.882	4.395

Then, the final reconstructed EC and MP profiles were obtained by averaging the previously determined profile variants. The values of errors $MAPE$, % for each of the four test EMF measurements separately for the MP and EC profiles are shown in Figure 3.

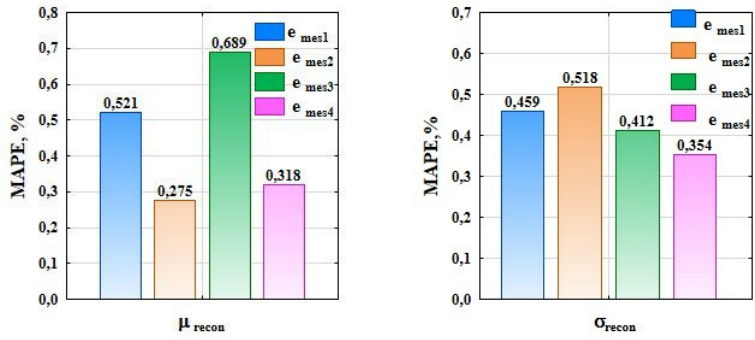

Figure 3. Errors $MAPE$, % for the MP and EC profiles separately for each of the four test EMF measurements. μ –(a) , σ –(b).

4 Discussion

Similar studies were performed with a priori consideration of the information in the metamodels only for EC and MP. An identical methodology was used in the numerical experiments. The results of profile identification at the excitation frequency $f = 2$ kHz in the active compact space were 0.352% for the MP profiles and 0.96% for the EC profiles [5].

Thus, the model calculations for the reconstruction of electrophysical profiles of planar TOs based on the results of direct measurements of the EMF amplitude and phase, presented in Table 6, indicate the effectiveness of the proposed methodology for simultaneous determination of profiles in one measurement when the metamodels take into account, in addition to electrophysical parameters, the frequencies at which measurements are made. Namely, evaluating the obtained values of the error $MAPE$, %, it can be noted that its value for the reconstructed MP profiles is in the range of $0.275\% \leq \text{MAPE}_\mu \leq 0.689\%$, and for the EC – $0.354\% \leq \text{MAPE}_\sigma \leq 0.518\%$. It should be noted that there is a tendency to reduce the errors in the reconstruction of EC profiles compared to studies where only two factors were taken into account in the metamodels at a fixed excitation frequency. This can probably be explained by a significant reduction in the number of search variables in the vectors of electrophysical parameters, which simplified the solution of the optimization problem by the stochastic method and increased the accuracy of its finding, despite some loss of information during the corresponding transformations of the search space. In addition, there is a pattern of a slight increase in errors for measuring MP profiles at high frequencies.

5 Conclusions

Thus, the study verifies the method for determining the electrophysical profiles of planar objects based on computer simulation of the eddy-current testing process, which is based on the apriori accumulation of information about them by modeling. The method involves solving an optimization problem using surrogate modeling techniques. The inverse problem of reconstructing the profiles of the EC and MP is solved, which consists in minimizing the quadratic target function in an active compact search subspace of reduced dimension. The method uses a heuristic bionic hybrid algorithm for finding a global extremum. The metamodels of the ECP are constructed on the basis of deep fully connected neural networks, which take into account, in addition to the electrophysical parameters of the TO, the frequencies at which measurements are possible. The accuracy of the metamodels is ensured by splitting the complex-valued neural network into two real-valued ones to approximate the real and imaginary parts of the ECP signal and by applying deep learning. The use of the PCA method made it possible to substantially simplify the conditions for finding the extremum by the optimization algorithm and obtain better solution values compared to the search in the full-factor space, despite some loss of a part of the complete information about the TO. Numerical experiments have proved the effectiveness of simultaneous reconstruction of the EC and MP profiles using additional information on multifrequency measurements, which made it possible to improve the accuracy of their determination as a result of a more thorough consideration of the interaction of the electromagnetic field of probe excitation with the TO.

References

[1] N. Bowler. *Eddy-current nondestructive evaluation.* Springer, New York, 2019. https://doi.org/10.1007/978-1-4939-9629-2.

[2] K.-T. Fang, M.-Q. Liu, H. Qin and Y.-D. Zhou. *Theory and application of uniform experimental designs*, volume 221. Springer, Singapore, 2018. https://doi.org/10.1007/978-981-13-2041-5.

[3] V. Halchenko, R. Trembovetska, C. Bazilo and N. Tychkova. Computer simulation of the process of profiles measuring of objects electrophysical parameters by surface eddy current probes. In E. Faure, O. Danchenko, M. Bondarenko, Y. Tryus, C. Bazilo and G. Zaspa(Eds.), *International Scientific-Practical Conference" Information Technology for Education, Science and Technics"*, pp. 411–424. Springer, Nature Switzerland, 2023. https://doi.org/10.1007/978-3-031-35467-0_25.

[4] V. Halchenko, R. Trembovetska, V. Tychkov and N. Tychkova. Construction of quasi-DOE on Sobol's sequences with better uniformity 2D projections. *Applied Computer Systems*, **28**(1):21–34, 2023. https://doi.org/10.2478/acss-2023-0003.

[5] V.Ya. Halchenko, R. Trembovetska, V. Tychkov and N. Tychkova. Surrogate methods for determining of profiles of material properties of planar test objects with accumulation of apriori information about them. *Archives of Electrical Engineering*, **73**(1):183–200, 2024. https://doi.org/10.24425/aee.2024.148864.

[6] V.Ya. Halchenko, R.V. Trembovetska and V.V. Tychkov. Surrogate synthesis of excitation systems for frame tangential eddy current probes. *Archives of Electrical Engineering*, **70**(4):743–757, 2021. https://doi.org/10.24425/aee.2021.138258.

[7] V.Ya. Halchenko, V.V. Tychkov, A.V. Storchak and R.V. Trembovetska. Reconstruction of surface radial profiles of electrophysical characteristics of cylindrical objects during eddy current measurements with a priori data. the selection formation for the surrogate model construction. *Ukrainskyi metrolohichnyi zhurnal*, **1**:35–50, 2020. https://doi.org/10.24027/2306-7039.1.2020.204226.

[8] V.Ya. Halchenko, A.N. Yakimov and D.L. Ostapuschenko. Global optimum search of functions with using of multiagent swarm optimization hybrid with evolutional composition formation of population. *Information technology*, **10**(170):9–16, 2010. Available on Internet: `http://novtex.ru/IT/it2010/It1010.pdf` (in Russian)

[9] J. Hampton, A. Fletcher, H. Tesfalem, A. Peyton and M. Brown. A comparison of non-linear optimization algorithms for recovering the conductivity depth profile of an electrically conductive block using eddy current inspection. *NDT & E International*, **125**:102571, 2022. https://doi.org/10.1016/j.ndteint.2021.102571.

[10] P. He, G.J Lin, M.-Q. Liu, Q. Xu and Y. Zhou. Theory and application of uniform designs. *SCIENTIA SINICA Mathematica*, **50**(5):561–570, 2020. https://doi.org/10.1360/SSM-2020-0065.

[11] P. Huang, J. Zhao, Z. Li, H. Pu, Y. Ding, L. Xu and Y. Xie. Decoupling conductivity and permeability using sweep-frequency eddy current method. *IEEE Transactions on Instrumentation and Measurement*, **72**:1–11, 2023. https://doi.org/10.1109/TIM.2023.3242017.

[12] Y.-Z. Lei. General series expression of eddy-current impedance for coil placed above multi-layer plate conductor. *Chinese Physics B*, **27**(6):060308, 2018. https://doi.org/10.1088/1674-1056/27/6/060308.

[13] M. Lu. *Forward and inverse analysis for non-destructive testing based on electromagnetic computation methods*. The University of Manchester, United Kingdom, 2018. Available on Internet: `https://pure.manchester.ac.uk/ws/portalfiles/portal/73361551/FULL_TEXT.PDF`

[14] H. Tesfalem, J. Hampton, A.D. Fletcher, M. Brown and A.J. Peyton. Electrical resistivity reconstruction of graphite moderator bricks from multi-frequency measurements and artificial neural networks. *IEEE Sensors Journal*, **21**(15):17005–17016, 2021. https://doi.org/10.1109/JSEN.2021.3080127.

[15] H. Tesfalem, A.J. Peyton, A.D. Fletcher, M. Brown and B. Chapman. Conductivity profiling of graphite moderator bricks from multifrequency eddy current measurements. *IEEE Sensors Journal*, **20**(9):4840–4849, 2020. https://doi.org/10.1109/JSEN.2020.2965201.

[16] T.P. Theodoulidis and E.E. Kriezis. *Eddy current canonical problems (with applications to nondestructive evaluation)*. Tech Science Press, 2006.

[17] R. Trembovetska, V. Halchenko and C. Bazilo. Inverse multi-parameter identification of plane objects electrophysical parameters profiles by eddy-current method. In O. Arsenyeva, T. Romanova, M. Sukhonos and Y. Tsegelnyk(Eds.), *International Conference on Smart Technologies in Urban Engineering*, pp. 202–212, Cham, 2023. Springer, Springer International Publishing. https://doi.org/10.1007/978-3-031-20141-7_19.

[18] S. Ullah, D.A. Nguyen, H. Wang, S. Menzel, B. Sendhoff and T. Bäck. Exploring dimensionality reduction techniques for efficient surrogate-assisted optimization. In *2020 IEEE Symposium Series on Computational Intelligence (SSCI)*, pp. 2965–2974. IEEE, 2020. https://doi.org/10.1109/SSCI47803.2020.9308465.

[19] E. Uzal. *Theory of eddy current inspection of layered metals*. Iowa State University, 1992. https://doi.org/10.31274/rtd-180813-9635.

[20] J. Wang, J. Zhou and X. Chen. *Data-Driven Fault Detection and Reasoning for Industrial Monitoring*. Springer Nature, Singapore, 2022. https://doi.org/10.1007/978-981-16-8044-1.

[21] Y. Wang, F. Sun and H. Xu. On design orthogonality, maximin distance, and projection uniformity for computer experiments. *Journal of the American Statistical Association*, **117**(537):375–385, 2020. https://doi.org/10.1080/01621459.2020.1782221.

[22] J. Xu, J. Wu, W. Xin and Z. Ge. Fast measurement of the coating thickness and conductivity using eddy currents and plane wave approximation. *IEEE Sensors Journal*, **21**(1):306–314, 2020. https://doi.org/10.1109/JSEN.2020.3014677.

[23] J. Xu, J. Wu, W. Xin and Z. Ge. Measuring ultrathin metallic coating properties using swept-frequency eddy-current technique. *IEEE Transactions on Instrumentation and Measurement*, **69**(8):5772–5781, 2020. https://doi.org/10.1109/TIM.2020.2966359.